International Journal of Mathematical Sciences and Optimization: Theory and Applications
10(3), 2024, Pages 10 - 30
https://doi.org/10.5281/zenodo.13152986

Application of Diffusion Magnetic Resonance Imaging Equation to Compressible and Incompressible Fluid Particles in a Spherical Region

A. Saba [1*], S. I. Yusuf [1], D. O. Olaoye [1], A. O. Jatto [1]

1. Department of Mathematics, Federal University of Technology, Minna, Niger State, Nigeria.
* Corresponding author: ahmedsabakpaki@gmail.com*, si.yusuf@futminna.edu.ng, metric60@gmail.com, ozijato@gmail.com

Article Info
Received: 23 July 2023 Revised: 25 November 2023
Accepted: 25 March 2024 Available online: 25 May 2024

Abstract

In the previous work, the response of viscous and non-viscous fluids to magnetic resonance was examined. In this research work, Diffusion magnetic resonance imaging, MRI, is used to study, analyse and compare the response of particles of compressible and incompressible fluids in a spherical region. The fluids considered are hydrogen gas and paraffin oil. The general flow equation was evolved from the fundamental Bloch equations. The general flow equation was solved using the method of separation of variables and applied to spherical region leading to Legendre equation of the first and second kinds. From the results obtained, it can be concluded that the value of Magnetization for hydrogen gas ranges from $9.28819444503 \times 10^{13}$ to 9.35×10^{14}. However, appreciable change can be noticed when magnetization is $9.2881944500003 \times 10^{13}$. For paraffin oil, the value of Magnetization ranges from $2.749305556000075 \times 10^{14}$ to 2.75×10^{14} with appreciable change noticed at magnetization value of $2.7493055560000094 \times 10^{14}$. The analytical solution of Diffusion MRI equation adopted in this research work has shown the difference in compressible (hydrogen gas) and incompressible (paraffin oil) fluids in a spherical region through the magnetization values that were generated. This is laying credence to the effectiveness and non-invasive properties of MRI.

Keywords: Spherical region, Compressible fluid, Incompressible fluid, Magnetization.
MSC2010: 37J40.

International Journal of Mathematical Sciences and Optimization: Theory and Applications
10(3), 2024, Pages 10 - 30
https://doi.org/10.5281/zenodo.13152986

1.0 Introduction

Felix Bloch and Edward Purcell discovered Nuclear Magnetic Resonance (NMR) independently in 1946 which gives them the Nobel Prize in physics. The fundamental phenomenon of nuclear magnetic resonance, NMR arises in atoms with odd number of protons or an odd number of neutrons. These atoms possess a feature called nuclear spin angular momentum that exhibits the NMR phenomenon. The foundation of NMR is the interaction of spins with the following magnetic fields: main static field , radio-frequency field and linear gradient fields as extracted from Nishimura [1].
Nuclear magnetic resonance techniques have been proved to be a powerful and reliable tool in studying flow in restricted geometries because it can provide self-diffusion coefficient accurately for the individual components or multi-component systems in a few minutes. Hence, it is particularly useful for studying diffusion, Dada *et al.*[2].
Singh and Srivastava [3] presented a numerical simulation of fractional-order and integer-order Bloch equations that occurs in NMR by using the Jacobi-polynomials. The numerical solution of the technique varies consistently at distinct values of fractional-order time derivatives and integer-order solutions of the technique were identical to the exact solution of the Bloch equations.
In another research, a simple and fast technique for solving the time dependent Bloch equations by using matrix operation method was derived by Murase and Tanki [4]. This method was validated in case of constant radio-frequency irradiation by comparing with the analytical solutions which indicates a good agreement between the methods.
Overtime, the nuclear in NMR was dropped as it was believed to connote dangerous nuclear energy released in significant amounts and the name MRI – Magnetic Resonance Imaging was adopted. MRI is a very powerful tool and has application in various aspects of human life especially in studying the behaviour of fluids generally. It is a method that has been applied severally by scientists and has proved to be very effective in revealing to minute details properties and activities of particles of fluids under consideration. Several scientists have applied MRI in carrying out a lot of investigation of fluid in the field of medicine, physics, radiology, oil and gas and so on, Awojoyogbe *et al.* [5].
MRI has also been further used to reveal the nature of the materials that can cause obstructions or blockage of fluids in a cylindrical pipe, Yusuf *et al.* [6].
Diffusion magnetic resonance imaging (DMRI) equation has been applied to study and analyse the discontinuities of flow of fluids in a symmetric cylindrical channel. In the work, it was shown that partial and total blockage could be determined using DMRI equation, Yusuf *et al.*[7]. Time dependent Bloch NMR flow equation was transformed to diffusion advection equation for the qualitative analysis of nuclear magnetization. The result obtained was used to study fluid flow in blood vessels under different bio-physico-geometrical conditions by Dada *et al.*[8]. Analytical solution of magnetic resonance imaging (MRI) equation was used to study and analyse the general behaviour of fluid flow in human living tissues, Yusuf *et al.* [9]. Another useful application of MRI was carried out with T1and T2 relaxation times from Bloch equations. These relaxation times were used to estimate the age of human organs, Olaoye *et al.* [10]. Yusuf *et al.* [11] also analysed partial and total blockage of unused engine oil in a radially symmetric cylindrical pipe using diffusion magnetic resonance equation. The analytical solutions of the transient solid-state diffusion of the single-phase and two-phase in radial spherical and cylindrical geometries were also considered. The modified differential equations were solved using error function method and obtained solutions used to analyse the diffusion interface position as a function of time and position in spheres and cylinders. The analytical solutions were validated with the results of a numerical approach called enthalpy method. The model was proved to be general, as far as, a semi-infinite solution for diffusion problems with

phase change exist in the form of error function that enables them to derive the exact closed-form of analytical solutions by updating the root at each radial position of the moving boundary interface, Ferreira *et al.* [12].

Datta and Pal [13] studied one dimensional radial diffusion equation in spherical coordinate system using the Lattice Boltzmann scheme. The scheme was investigated and there was a great analogy between the simulation and the analytical solution. The result obtained shows that the scheme will be able to simulate the radial diffusion equation accurately. Gharehbaghi [14] developed a numerical model based on the Finite Volume Method to predict a time dependent one-dimensional advection diffusion equation with variable coefficient in a semi-finite domain. The third and fourth order schemes were used to solve the governing equations. Two dispersion problems were used to simulate various conditions as first solute dispersion along steady flow through inhomogeneous domain and secondly solute dispersion along temporarily dependent unsteady flow through inhomogeneous domain. Then, the results of third-order and fourth-order Finite Volume Method (FVM) were more accurate than the result of quick scheme FVM and among the three approaches, the fourth order FVM was achieved to present the best predictions.

Belyaev *et al.* [15] investigated two dimensional variables of fluid particles of motion in a curved duct using numerical analysis. Navier-Stoke's equation was used to model the phenomenon. Control Volume (CV) approach was used to discretize the initial equations. The result discovered shows that the trajectory of the moisture reduces the motion and its speed.

In the work of Fatumbi and Fenuga [16], reference was made to micro-polar fluids which represent fluids consisting of rigid, randomly oriented (or spherical) particles suspended in a viscous medium, where particles deformation is ignored. These are group of fluids with non-symmetric stress tensor that are called polar fluids which constitute a substantial generalization of the Navier-Stoke's model. These fluids offer a mathematical model for investigating the flow of complex and complicated fluids such as suspension solution, animal blood, liquid crystals, polymeric fluids and clouds with dust. Similarly, Isede *et al.* [17] pioneered the classical unidirectional laminar flow problem of an incompressible and viscous electrically conductive fluid permeated by a non-varying magnetic field; applied transversely to the parallel walls of the channel. Popoola *et al.*[18] examined the two-dimensional steady flow of heat and mass transfer in an incompressible magneto hydrodynamic viscous-elastic fluid pass a stretching sheet in the presence of thermal diffusion and chemical reaction. The similarity transformation method was used to convert the partial differential equations governing the flow of heat and mass transfer properties into the coupled ordinary differential equations.

Eli and Aboh [19] considered the advective-NMR model of the blood vessels with changing dimensions. The aim was to write a programme on the solution of diffusion-advection equation in cylindrical coordinate with variable diffusion coefficient that was obtained. The programme was developed in java language. Then by the java technique, the simulation of software has developed with an object-oriented approach was nicely separated. It was observed that a little change on the cross-sectional value makes versed change on the blood flow rate.

Mallin *et al.* [20] & Olaide *et al.* [21] also applied NMR pulse to determine the properties of glycerine and mineral oil. The application of nuclear magnetic resonance measurement in petroleum industry gives better understanding of the interaction between fluids in the reservoirs and rock properties and one of the best tools for quantifying fluid properties, reservoir properties as well as determining reservoir productivity.

Available literature show that several works have been carried out in the field of fluid flow using Magnetic Resonance Imaging (MRI) in rectangular and cylindrical media as well as across plates

International Journal of Mathematical Sciences and Optimization: Theory and Applications
10(3), 2024, Pages 10 - 30
https://doi.org/10.5281/zenodo.13152986

but very few authors have worked on spherical medium. However, most fluids in earth crust or rocks are situated approximately in spherical medium which is the motivation to carry out this present work. This research work is aimed at providing an analytical solution of the general flow equation evolved from the Bloch NMR equations with a view to studying the response of fluid particles in spherical region using diffusion magnetic resonance imaging equation. Therefore, this research work examined the difference in response of compressible (hydrogen gas) and incompressible (paraffin oil) fluids in a spherical region.

2.0 Mathematical Formulation

The Bloch equations are given as:

$$\frac{dM}{dt} = -\frac{M_x}{T_2} \tag{1}$$

$$\frac{dM}{dt} = \gamma M_z \beta_1 - \frac{M_y}{T_2} \tag{2}$$

$$\frac{dM}{dt} = -\gamma M_y \beta_1(x) + \frac{M_0 - M_z}{T_1} \tag{3}$$

where
M_x = Component of transverse magnetization along x- axis (dimensionless)
M_y = Component of transverse magnetization along y- axis (dimensionless)
M_z = Component of magnetization along z- axis (dimensionless)
M_0 = Equilibrium magnetization (dimensionless)
γ = Gyro-magnetic ratio of fluid spins - $(radT^{-1}s^{-1})$
β_1 = Radio-frequency (RF) magnetic field -(Tesla,T)
T_1 = Longitudinal or spin lattice relaxation time -(ms)
T_2 = Transversal or spin-spin relaxation time -(ms)
v = The fluid velocity - (sec)
t = time - (sec)
In applying the Bloch NMR equations, the following assumptions were made:

i The fluid is assumed to be magnetized by an external magnetic field,B_0, called static magnetic field along the laboratory Z–direction to an equilibrium magnetization M_0 before entering the exit coil.

ii The radiofrequency excitation filed B_1 is applied along X-laboratory direction.

iii The z-axis in the rotating frame coincides with the laboratory Z-axis.

iv The x-axis makes an angle (ωt) at any instant time (t) with the laboratory X-axis.

v Under the influence of environmental interaction, the x, y and z components of magnetization relaxes with the relaxation times T_1 and T_2, Nishimura [1]

International Journal of Mathematical Sciences and Optimization: Theory and Applications
10(3), 2024, Pages 10 - 30
https://doi.org/10.5281/zenodo.13152986

From the Bloch equations, the general equation for fluid flow was evolved by Awojoyogbe [22]:

$$\implies v^2\frac{\partial^2 M_y}{\partial x^2}+2v\frac{\partial^2 M_y}{\partial x\partial t}+vT_0\frac{\partial M_y}{\partial x}+T_0\frac{\partial M_y}{\partial t}+\frac{\partial^2 M_y}{\partial t^2}+(T_q+\gamma^2\beta_1^2(x,t))M_y=F_0\gamma\beta_1(x,t) \quad (4)$$

where
$T_0=\frac{1}{T_2}+\frac{1}{T_1}$, $T_q=\frac{1}{T_1T_2}$ and $F_0=\frac{M_0}{T_1}$
From equation (4), assuming that each of the terms extracted and listed in equation (5) is set to zero:

$$\frac{\partial^2 M_y}{\partial t^2}+2v\frac{\partial^2 M_y}{\partial x\partial t}+vT_0\frac{\partial M_y}{\partial x}+(T_q+\gamma^2\beta_1^2(x,t))M_y=0 \quad (5)$$

Then, equation (4) reduces to:

$$v^2\frac{\partial^2 M_y}{\partial x^2}+T_0\frac{\partial M_y}{\partial t}=F_0\gamma\beta_1(x,t) \quad (6)$$

$$\implies \frac{\partial M_y}{\partial t}=-\frac{v^2}{T_0}\frac{\partial^2 M_y}{\partial x^2}+\frac{F_0}{T_0}\gamma\beta_1(x,t) \quad (7)$$

Let $-\frac{v^2}{T_0}=D$, then equation (7) becomes:

$$\frac{\partial M_y}{\partial t}=D\frac{\partial^2 M_y}{\partial x^2}+\frac{F_0}{T_0}\gamma\beta_1(x,t) \quad (8)$$

Hence, the parameter D, is called diffusion coefficient that is accurately defined in terms of MRI fluid flow which is an intrinsic part of the Bloch nuclear magnetic resonance equation. Its unit is m^2s^{-1}. The function $\frac{F_0}{T_0}\gamma\beta_1(x,t)$ is called forcing function.
In 3-Dimension, equation (8) becomes:

$$\frac{\partial M_y}{\partial t}=D\left(\frac{\partial^2 M_y}{\partial x^2}+\frac{\partial^2 M_y}{\partial y^2}+\frac{\partial^2 M_y}{\partial z^2}\right)+\frac{F_0}{T_0}\gamma\beta_1(x,t) \quad (9)$$

In spherical coordinates system defined as (r,θ,ϕ) using $x=rsin\theta cos\phi$, $y=rsin\theta sin\phi$ and $z=rcos\theta$ with $r=\sqrt{x^2+y^2+z^2}=(x^2+y^2+z^2)^{\frac{1}{2}}$ $cos\theta=\frac{z}{r}=\frac{z}{(x^2+y^2+z^2)^{\frac{1}{2}}}$ and $tan\phi=\frac{y}{x}=\frac{sin\phi}{cos\phi}$, equation (9) becomes:

$$\frac{\partial M_y}{\partial t}=D\left\{\frac{1}{r^2}\frac{\partial}{\partial r}\left(r^2\frac{\partial M_y}{\partial r}\right)+\frac{1}{r^2\sin\theta}\frac{\partial}{\partial\theta}\left(\sin\theta\frac{\partial M_y}{\partial\theta}\right)+\frac{1}{r^2\sin^2\theta}\frac{\partial^2 M_y}{\partial\phi^2}\right\}+\frac{F_0}{T_0}\gamma\beta_1(t) \quad (10)$$

Assuming that $M_y=M_y(r,\theta,t)$, then $\frac{\partial^2 M_y}{\partial\phi^2}=0$ this implies that the particles of the fluid align in the same z − direction upon introduction of magnetic field which makes the particles exhibit constant or uniform motion. Consequently, equation (10) reduces to:

$$\frac{\partial M_y}{\partial t}=D\left\{\frac{1}{r^2}\frac{\partial}{\partial r}\left(r^2\frac{\partial M_y}{\partial r}\right)+\frac{1}{r^2\sin\theta}\frac{\partial}{\partial\theta}\left(\sin\theta\frac{\partial M_y}{\partial\theta}\right)\right\}+\frac{F_0}{T_0}\gamma\beta_1(t) \quad (11)$$

Applying the method of separation of variables and substituting $M_y=R(r)F(\theta)$.
The terms in the brackets on the righthand side of equation (11) are as follows:

$$\frac{1}{r^2}\frac{d}{dr}\left(r^2\frac{d\left(R(r)F(\theta)\right)}{dr}\right)+\frac{1}{r^2\sin\theta}\frac{d}{d\theta}\left(\sin\theta\frac{d\left(R(r)F(\theta)\right)}{d\theta}\right)=0 \quad (12)$$

$$\implies \frac{F(\theta)}{r^2}\frac{d}{dr}\left(r^2\frac{dR(r)}{dr}\right)+\frac{R(r)}{r^2\sin\theta}\frac{d}{d\theta}\left(\sin\theta\frac{dF(\theta)}{d\theta}\right)=0 \tag{13}$$

Then, multiplying equation (13) by $\dfrac{r^2}{R(r)F(\theta)}$ gives; (14)

$$\implies \frac{1}{R(r)}\frac{d}{dr}\left(r^2\frac{dR(r)}{dr}\right)=-\frac{1}{F(\theta)\sin\theta}\frac{d}{d\theta}\left(\sin\theta\frac{dF(\theta)}{d\theta}\right) \tag{15}$$

Since the left-hand side of equation (15) depends only on r and the right-hand side also depends only on θ, then each side must be equal to a constant (say $-k^2$):

$$\implies \frac{1}{R(r)}\frac{d}{dr}\left(r^2\frac{dR(r)}{dr}\right)=-\frac{1}{F(\theta)\sin\theta}\frac{d}{d\theta}\left(\sin\theta\frac{dF(\theta)}{d\theta}\right)=-k^2 \tag{16}$$

So, the following equations are obtained from equation (16) as:

$$\frac{1}{R(r)}\frac{d}{dr}\left(r^2\frac{dR(r)}{dr}\right)=-k^2 \tag{17}$$

$$\frac{1}{F(\theta)\sin\theta}\frac{d}{d\theta}\left(\sin\theta\frac{dF(\theta)}{d\theta}\right)=k^2 \tag{18}$$

Now, solving equation (17) which can also be expressed as:

$$r^2\frac{d^2R(r)}{dr^2}+2r\frac{dR(r)}{dr}+k^2R(r)=0 \tag{19}$$

Then, let the solution of equation (19) be of the form:

$$R(r)=r^P \tag{20}$$

$$\implies \frac{dR(r)}{dr}=Pr^{P-1} \tag{21}$$

$$\implies \frac{d^2R(r)}{dr^2}=P(P-1)r^{P-2} \tag{22}$$

Substituting equation (20), (21) and (22) into equation (19) gives:

$$r^2\left(P(P-1)r^{P-2}\right)+2r(Pr^{P-1})+k^2r^P=0 \tag{23}$$

$$\implies (P^2-P)r^P+2Pr^P+k^2r^P=0 \tag{24}$$

$$\implies (P^2+P+k^2)r^P=0 \tag{25}$$

This follows that if $r^P\neq 0$, then

$$P^2+P+k^2=0 \tag{26}$$

$$\implies P = \frac{-1}{2} + \sqrt{\frac{1}{4} - k^2} \text{ or } P = \frac{-1}{2} - \sqrt{\frac{1}{4} - k^2} \tag{27}$$

Then, substituting equation (27) into equation (20), gives:

$$R(r) = A_1 r^{\frac{-1}{2}+\sqrt{\frac{1}{4}-k^2}} + B_1 r^{\frac{-1}{2}-\sqrt{\frac{1}{4}-k^2}} \tag{28}$$

where A_1 and B_1 are two arbitrary constants
So, let

$$\frac{-1}{2} + \sqrt{\frac{1}{4} - k^2} = n \tag{29}$$

and

$$\frac{-1}{2} - \sqrt{\frac{1}{4} - k^2} = -n - 1 \tag{30}$$

Then, substituting equations (29) and (30) into equation (28) gives:

$$R(r) = A_1 r^n + B_1 r^{-n-1} \tag{31}$$

$$\implies R(r) = A_1 r^n + \frac{B_1}{r^{n+1}} \tag{32}$$

Now, multiplying equation (29) by (30) and simplifying yields:

$$k^2 = -n(n+1) \tag{33}$$

Now, considering equation (18) and substituting equation (33) into it, gives:

$$\frac{1}{F(\theta)\sin\theta}\frac{d}{d\theta}\left(\sin\theta\frac{dF(\theta)}{d\theta}\right) = -n(n+1) \tag{34}$$

$$\implies \frac{d}{d\theta}\left(\sin\theta\frac{dF(\theta)}{d\theta}\right) + n(n+1)\sin\theta F(\theta) = 0 \tag{35}$$

To transform equation (35) to Legendre equation,
Let $\eta = \cos\theta$, then:

$$\frac{dF(\theta)}{d\theta} = \frac{dF(\theta)}{d\eta}\cdot\frac{d\eta}{d\theta} \tag{36}$$

$$\left.\begin{aligned} \sin\theta\tfrac{dF(\theta)}{d\theta} &= \sin\theta\tfrac{dF(\theta)}{d\eta}\cdot\tfrac{d\eta}{d\theta} \\ \tfrac{d}{d\theta} &= \tfrac{d}{d\eta}\cdot\tfrac{d\eta}{d\theta} \end{aligned}\right\} \tag{37}$$

But $\frac{d\eta}{d\theta} = -\sin\theta$, then equation (37) becomes:

$$\left.\begin{aligned} \sin\theta\tfrac{dF(\theta)}{d\theta} &= -\sin^2\theta\tfrac{dF(\theta)}{d\eta} \\ \tfrac{d}{d\theta} &= -\sin\theta\tfrac{d}{d\eta} \end{aligned}\right\} \tag{38}$$

International Journal of Mathematical Sciences and Optimization: Theory and Applications
10(3), 2024, Pages 10 - 30
https://doi.org/10.5281/zenodo.13152986

Then, substituting equation (38) into equation (35) gives:

$$\frac{d}{d\eta}\left(-\sin^2\theta\frac{dF(\theta)}{d\eta}\right)(-\sin\theta)+n(n+1)\sin\theta F(\theta)=0 \tag{39}$$

Multiplying equation (39) by $\frac{1}{\sin\theta}$ we have:

$$\implies \frac{d}{d\eta}\left(\sin^2\theta\frac{dF(\theta)}{d\eta}\right)+n(n+1)F(\theta)=0 \tag{40}$$

But recall that $\sin^2\theta+\cos^2\theta=1 \implies \sin^2\theta=1-\cos^2\theta=(1-\eta^2)$, then equation (40) becomes:

$$\frac{d}{d\eta}\left((1-\eta^2)\frac{dF(\theta)}{d\eta}\right)+n(n+1)F(\theta)=0 \tag{41}$$

Now, let $\eta=x$ and $F(\theta)=y$ then equation (41) becomes:

$$\frac{d}{dx}\left((1-x^2)\frac{dy}{dx}\right)+n(n+1)y=0 \tag{42}$$

$$\implies (1-x^2)\frac{d^2y}{dx^2}-2x\frac{dy}{dx}+n(n+1)y=0 \tag{43}$$

Applying Frobenius method to solve equation (43), let the series solution of equation (43) be in the form:

$$y=\sum_{q=0}^{\infty}a_qx^{q+c}=x^c\left\{a_0+a_1x+a_2x^2+a_3x^3+a_4x^4+a_5x^5+...\right\} \tag{44}$$

$$\implies \frac{dy}{dx}=\sum_{q=0}^{\infty}(q+c)a_kx^{q+c-1} \tag{45}$$

$$\implies \frac{d^2y}{dx^2}=\sum_{q=0}^{\infty}(q+c)(q+c-1)a_qx^{q+c-2} \tag{46}$$

Then, substituting equation (44), (45) and (46) into equation (43) gives:

$$\left.\begin{array}{l}(1-x^2)\sum_{q=0}^{\infty}(q+c)(q+c-1)a_qx^{q+c-2}-2x\sum_{q=0}^{\infty}(q+c)a_qx^{q+c-1}+\\ n(n+1)\sum_{q=0}^{\infty}a_qx^{q+c}=0\end{array}\right\} \tag{47}$$

$$\left.\begin{array}{l}\implies \sum_{q=0}^{\infty}(q+c)(q+c-1)a_qx^{q+c-2}-\sum_{q=0}^{\infty}(q+c)(q+c-1)a_qx^{q+c}-\\ \sum_{q=0}^{\infty}2(q+c)a_qx^{q+c}+n(n+1)\sum_{q=0}^{\infty}a_qx^{q+c}=0\end{array}\right\} \tag{48}$$

$$\left.\begin{array}{l}\implies \sum_{q=0}^{\infty}(q+c)(q+c-1)a_qx^{q+c-2}-\sum_{q=0}^{\infty}\left\{((q+c)(q+c-1)+2(q+c)-n(n+1))a_q\right\}x^{q+c}\\ =0\end{array}\right\} \tag{49}$$

Evaluating x^{q+c-2} at $q=0$ and $q=1$,

$$\left.\begin{array}{l} c(c-1)a_0x^{c-2}+c(c+1)a_1x^{c-1}+\sum_{q=2}^{\infty}(q+c)(q+c-1)a_qx^{q+c-2}- \\ \sum_{q=0}^{\infty}\left\{((q+c)(q+c+1)-n(n+1))a_q\right\}x^{q+c}=0 \end{array}\right\} \tag{50}$$

Also equating the coefficients of x^{c-2} and x^{c-1} in equation (50) gives:

$$\left[x^{c-2}\right]: c(c-1)a_0=0,\ \text{if } a_0\neq 0 \tag{51}$$

Then, $c=0$ or $c=1$ {are called indicial roots}

$$\left[x^{c-1}\right]: c(c+1)a_1=1 \tag{52}$$

Then, for $c=0$, a_1 is undefined
and for $c=1$, $a_1=0$ Now, equation (50) is reduced to:

$$\sum_{q=2}^{\infty}(q+c)(q+c-1)a_qx^{q+c-2}-\sum_{q=0}^{\infty}\left\{((q+c)(q+c+1)-n(n+1))a_q\right\}x^{q+c}=0 \tag{53}$$

Then, from the first term of equation (53) let $q=q+2$ yields;

$$\sum_{q=0}^{\infty}(q+c+2)(q+c+1)a_{q+2}x^{q+c}-\sum_{q=0}^{\infty}\left\{((q+c)(q+c+1)-n(n+1))a_q\right\}x^{q+c}=0 \tag{54}$$

Now, equating the coefficient of x^{q+c} in equation (54) yields:

$$(q+c+2)(q+c+1)a_{q+2}-((q+c)(q+c+1)-n(n+1))a_q=0 \tag{55}$$

Considering the value of $c=0$ in equation (55), gives:

$$(q+2)(q+1)a_{q+2}-(q(q+1)-n(n+1))a_q=0 \tag{56}$$

$$\implies (q+2)(q+1)a_{q+2}=(q-n)(n+q+1))a_q \tag{57}$$

$$\implies a_{q+2}=\frac{-(n-q)(n+q+1)a_q}{(q+2)(q+1)};\ \text{for } q=0,1,2... \tag{58}$$

Now, putting the values of q into equation (58) the following are obtained:

$$\text{For } q=0,\ a_2=\frac{-n(n+1)a_0}{2\cdot 1}=\frac{-n(n+1)a_0}{2!} \tag{59}$$

$$\text{For } q=1,\ a_3=\frac{-(n-1)(n+2)a_1}{3\cdot 2}=\frac{-(n-1)(n+2)a_1}{3!} \tag{60}$$

$$\text{For } q=2,\ a_4=\frac{-(n-2)(n+3)a_2}{4\cdot 3}=\frac{n(n-2)(n+1)(n+3)a_0}{4!} \tag{61}$$

$$\text{For } q=3,\ a_5=\frac{-(n-3)(n+4)a_3}{5\cdot 4}=\frac{(n-1)(n-3)(n+2(n+4))a_1}{5!} \tag{62}$$

The process continues in that order.
Also, substituting equation (59), (60), (61) and (62) into equation (44) and collecting the like terms, for $c=0$ gives:

$$\left.\begin{aligned} y=a_0\left(1-\tfrac{n(n+1)}{2!}x^2+\tfrac{n(n-2)(n+1)(n+3)}{4!}x^4+...\right)+ \\ a_1\left(x-\tfrac{(n-1)(n+2)}{3!}x^3+\tfrac{(n-1)(n-3)(n+2)(n+4)}{5!}x^5+...\right)\end{aligned}\right\} \tag{63}$$

Then, equation (63) can also be expressed as:

$$y=A_2P_n(x)+B_2Q_n(x) \tag{64}$$

where, A_2 and B_2 are two arbitrary constants,

$$\left.\begin{aligned} P_n(x)=a_0\left(1-\tfrac{n(n+1)}{2!}x^2+\tfrac{n(n-2)(n+1)(n+3)}{4!}x^4+...\right) \\ Q_n(x)=a_1\left(x-\tfrac{(n-1)(n+2)}{3!}x^3+\tfrac{(n-1)(n-3)(n+2)(n+4)}{5!}x^5+...\right)\end{aligned}\right\} \tag{65}$$

But recall that $F(\theta)=y$ and $\eta=x$, then equation (64) becomes:

$$F(\theta)=A_2P_n(\eta)+B_2Q_n(\eta),\ \text{where } \eta=\cos\theta \tag{66}$$

Thus, substituting equations (32) and (66) into equation (11), gives the general solution as:

$$M_y(r,\theta,t)=D\left\{\left(A_1r^n+\frac{B_1}{r^{n+1}}\right)(A_2P_n(\eta)+B_2Q_n(\eta))\right\}+\int_0^{t_1}\frac{F_0}{T_0}\gamma\beta_1(t)dt \tag{67}$$

where the functions $P_n(\eta)$ and $Q_n(\eta)$ are the Legendre functions of the first and second kinds and the function $\int_0^{t_1}\frac{F_0}{T_0}\gamma\beta_1(t)dt$ is the radio-frequency field applied to perturb the molecules of the fluid. Since M_y must be bounded at $\theta=0$ and π, either $\eta=\pm1$, let choose $B_2=0$ in equation (67), then the bounded solution is obtained as:

$$M_y(r,\theta,t)=D\left\{\left(Ar^n+\frac{B}{r^{n+1}}\right)P_n(\eta)\right\}+\int_0^{t_1}\frac{F_0}{T_0}\gamma\beta_1(t)dt \tag{68}$$

Then, the boundary conditions to be imposed are:

$$M_y=\begin{cases} M_0,\ \text{if } 0<\theta<\frac{\pi}{2},\ \text{i.e. } 0<\eta<1 \\ 0,\ \text{if } \frac{\pi}{2}<\theta<\pi,\ \text{i.e. } -1<\eta<0\end{cases} \tag{69}$$

and M_y is bounded.
Since M_y is bounded at $r=0$, choosing $B=0$ in equation (68) it gives:

$$M_y(r,\theta,t)=DAr^nP_n(\eta)+\int_0^{t_1}\frac{F_0}{T_0}\gamma\beta_1(t)dt \tag{70}$$

International Journal of Mathematical Sciences and Optimization: Theory and Applications
10(3), 2024, Pages 10 - 30
https://doi.org/10.5281/zenodo.13152986

Now, replacing A by A_n and applying superposition principle in equation (70) yields:

$$M_y(r,\theta,t) = D\sum_{n=0}^{\infty} A_n r^n P_n(\eta) + \int_0^{t_1} \frac{F_0}{T_0}\gamma\beta_1(t)dt \tag{71}$$

$$\left.\begin{array}{l}\implies M_y(r,\theta,t) = D[A_0P_0(\cos\theta) + A_1rP_1(\cos\theta) + A_2r^2P_2(\cos\theta) + A_3r^3P_3(\cos\theta) + \\ A_4r^4P_4(\cos\theta) + A_5r^5P_5(\cos\theta) + ...] + \int_0^{t_1} \frac{F_0}{T_0}\gamma\beta_1(t)dt\end{array}\right\} \tag{72}$$

where $\eta = \cos\theta$ Then, from equation (72) considering:

$$M_y(r,\theta) = \sum_{n=0}^{\infty} A_n r^n P_n(\eta) \tag{73}$$

So, when $r = 1$ then equation (73) becomes:

$$M_y(1,\theta) = \sum_{n=0}^{\infty} A_n P_n(\eta) \tag{74}$$

Now, by the orthogonality of Legendre polynomials and multiplying both sides by $P_m(\eta)$ and integrating from $(-1,1)$ then equation (74) becomes:

$$\int_{-1}^{1} M_y(1,\theta)P_m(\eta)d\eta = \sum_{n=0}^{\infty}\sum_{m=0}^{\infty} A_n \int_{-1}^{1} P_n(\eta)P_m(\eta)d\eta \tag{75}$$

Then, if $n = m$ and $\eta = x$ equation (75) becomes:

$$\int_{-1}^{1} M_y(1,\theta)P_n(x)dx = \sum_{n=0}^{\infty} A_n \int_{-1}^{1} [P_n(x)]^2 dx \tag{76}$$

Recall from the generating functions of Legendre polynomials given by

$$\sum_{n=0}^{\infty} P_n(x)t^n = (1 - 2xt + t^2)^{\frac{-1}{2}} \tag{77}$$

$$\sum_{m=0}^{\infty} P_m(x)t^m = (1 - 2xt + t^2)^{\frac{-1}{2}} \tag{78}$$

Then, multiplying equation (77) by (78) gives:

$$\implies \sum_{m=0}^{\infty}\sum_{n=0}^{\infty} P_m(x)P_n(x)t^{m+n} = (1 - 2xt + t^2)^{-1} \tag{79}$$

Now, if $m = n$ and integrating both sides from $(-1,1)$ with respect to x gives:

$$\implies \sum_{n=0}^{\infty}\int_{-1}^{1} [P_n(x)]^2 t^{2n} dx = \int_{-1}^{1} \left[\frac{1}{1 - 2xt + t^2}\right] dx \tag{80}$$

IJMSO

International Journal of Mathematical Sciences and Optimization: Theory and Applications
10(3), 2024, Pages 10 - 30
https://doi.org/10.5281/zenodo.13152986

$$\implies \sum_{n=0}^{\infty}\int_{-1}^{1}[P_n(x)]^2t^{2n}dx = \left[\frac{\log(1-2xt+t^2)}{-2t}\right]_{-1}^{1} \tag{81}$$

$$\implies \sum_{n=0}^{\infty}\int_{-1}^{1}[P_n(x)]^2t^{2n}dx = \frac{-1}{2t}\left[\log(1-2t+t^2)-\log(1+2t+t^2)\right] \tag{82}$$

$$\implies \sum_{n=0}^{\infty}\int_{-1}^{1}[P_n(x)]^2t^{2n}dx = \frac{-1}{2t}\left[\log(1-t)^2-\log(1+t)^2\right] \tag{83}$$

$$\implies \sum_{n=0}^{\infty}\int_{-1}^{1}[P_n(x)]^2t^{2n}dx = \frac{-1}{t}\left[\frac{2}{2}\log(1-t)-\frac{2}{2}\log(1+t)\right] \tag{84}$$

$$\implies \sum_{n=0}^{\infty}\int_{-1}^{1}[P_n(x)]^2t^{2n}dx = \frac{1}{t}\left[\log(1+t)-\log(1-t)\right] \tag{85}$$

But recall that;

$$\left.\begin{array}{l} \log(1+t) = t-\frac{t^2}{2}+\frac{t^3}{3}-\frac{t^4}{4}+\frac{t^5}{5}-... \\ \log(1-t) = -\left[t+\frac{t^2}{2}+\frac{t^3}{3}+\frac{t^4}{4}+\frac{t^5}{5}+...\right] \end{array}\right\} \tag{86}$$

Then equation (85) becomes:

$$\therefore \sum_{n=0}^{\infty}\int_{-1}^{1}[P_n(x)]^2t^{2n}dx = \frac{1}{t}\left[t-\frac{t^2}{2}+\frac{t^3}{3}-\frac{t^4}{4}+\frac{t^5}{5}-...+t+\frac{t^2}{2}+\frac{t^3}{3}+\frac{t^4}{4}+\frac{t^5}{5}+...\right] \tag{87}$$

$$\implies \sum_{n=0}^{\infty}\int_{-1}^{1}[P_n(x)]^2t^{2n}dx = \frac{2t}{t}\left[1+\frac{t^2}{3}+\frac{t^4}{5}+...\right] \tag{88}$$

$$\implies \sum_{n=0}^{\infty}\int_{-1}^{1}[P_n(x)]^2t^{2n}dx = 2\left[\frac{t^{2n}}{2n+1}\right],\ \text{for } n=0,1,2,... \tag{89}$$

$$\therefore \sum_{n=0}^{\infty}\int_{-1}^{1}[P_n(x)]^2t^{2n}dx = \frac{2t^{2n}}{2n+1} \tag{90}$$

Then, equating the coefficients of t^{2n} gives;

$$\sum_{n=0}^{\infty}\int_{-1}^{1}[P_n(x)]^2dx = \frac{2}{2n+1} \tag{91}$$

Now, substituting equation (91) into equation (76), obtained:

$$\int_{-1}^{1}M_y(1,\theta)P_n(x)dx = \frac{2A_n}{2n+1} \tag{92}$$

Then, making A_n the subject in equation (92) gives:

$$A_n = \frac{2n+1}{2}\int_{-1}^{1}M_y(1,\theta)P_n(x)dx,\ \text{for } n=0,1,2,... \tag{93}$$

Applying boundary conditions to equation (93) gives:

$$A_n = \frac{2n+1}{2}\int_0^1 M_0 P_n(x)dx + \frac{2n+1}{2}\int_{-1}^0 (0)P_n(x)dx \tag{94}$$

$$A_n = \frac{(2n+1)M_0}{2}\int_0^1 P_n(x)dx \tag{95}$$

Now, putting $n = 0, 1, 2, 3, 4, 5, ...$ into equation (95) yields the following:

$$\text{For } n = 0 : A_0 = \frac{1}{2}M_0\int_0^1 P_0(x)dx = \frac{M_0}{2}\int_0^1 (1)dx = \frac{M_0}{2} \tag{96}$$

$$\text{For } n = 1 : A_1 = \frac{3}{2}M_0\int_0^1 P_1(x)dx = \frac{3M_0}{2}\int_0^1 xdx = \frac{3M_0}{4} \tag{97}$$

$$\text{For } n = 2 : A_2 = \frac{5}{2}M_0\int_0^1 P_2(x)dx = \frac{5M_0}{2}\int_0^1 \frac{1}{2}(3x^2-1)dx = 0 \tag{98}$$

$$\text{For } n = 3 : A_3 = \frac{7}{2}M_0\int_0^1 P_3(x)dx = \frac{7M_0}{2}\int_0^1 \frac{1}{2}(5x^3-3x)dx = \frac{-7M_0}{16} \tag{99}$$

$$\text{For } n = 4 : A_4 = \frac{9}{2}M_0\int_0^1 P_4(x)dx = \frac{9M_0}{2}\int_0^1 \frac{1}{8}(35x^4-30x^2+3)dx = 0 \tag{100}$$

$$\text{For } n = 5 : A_5 = \frac{11}{2}M_0\int_0^1 P_5(x)dx = \frac{11M_0}{2}\int_0^1 \frac{1}{8}(63x^5-70x^3+15x)dx = \frac{11M_0}{32} \tag{101}$$

The process continues in that order.
Now, substituting equation (96), (97), (98), (99), (100 and (101) into equation (72) gives:

$$\left.\begin{array}{l} M_y(r,\theta,t) = D[\frac{M_0}{2}P_0(\cos\theta) + \frac{3M_0}{4}rP_1(\cos\theta) - \frac{7M_0}{16}r^3P_3(\cos\theta)+ \\ \frac{11M_0}{32}r^5P_5(\cos\theta) + ...] + \int_0^{t_1}\frac{F_0}{T_0}\gamma\beta_1(t)dt \end{array}\right\} \tag{102}$$

Hence, the solution of the magnetization M_y is:

$$\left.\begin{array}{l} M_y(r,\theta,t) = \frac{DM_0}{2}[1 + \frac{3}{2}rP_1(\cos\theta) - \frac{7}{8}r^3P_3(\cos\theta) + \frac{11}{16}r^5P_5(\cos\theta) + ... \\ \frac{11M_0}{32}r^5P_5(\cos\theta) + ...] + \int_0^{t_1}\frac{F_0}{T_0}\gamma\beta_1(t)dt \end{array}\right\} \tag{103}$$

Now, solving the integral in equation (103) as follows:

$$\frac{F_0}{T_0}\gamma\int_0^{t_1}\beta_1(t)dt \tag{104}$$

$$\frac{F_0}{T_0}\gamma\int_0^{t_1}\beta_1(t)dt = \left[\frac{F_0}{T_0}\gamma\beta_1(t)\right]_0^{t_1} \tag{105}$$

$$\implies \frac{F_0}{T_0}\gamma\int_0^{t_1}\beta_1(t)dt = \frac{F_0}{T_0}\gamma\beta_1(t_1) \tag{106}$$

A radio-frequency pulse $\beta_1(t_1)$ is needed to transmit energy to the sample of fluid considered in the sphere in order to activate the nuclei so that they emit signal.
But recall that: $F_0 = \frac{M_0}{T_1}$ and $T_0 = \frac{1}{T_2} + \frac{1}{T_1} = \frac{T_1+T_2}{T_1T_2}$ Then, equation (106) becomes:

$$\frac{F_0}{T_0}\gamma \int_0^{t_1} \beta_1(t)dt = \frac{M_0}{T_1} \times \frac{T_1T_2}{T_1+T_2}\gamma\beta_1(t_1) \tag{107}$$

$$\implies \frac{F_0}{T_0}\gamma \int_0^{t_1} \beta_1(t)dt = \frac{T_2M_0\gamma}{T_1+T_2}\beta_1(t_1) \tag{108}$$

Therefore,

$$M_y(r,\theta,t) = \left.\begin{array}{l} \frac{DM_0}{2}\left[1 + \frac{3}{2}rP_1(\cos\theta) - \frac{7}{8}r^3P_3(\cos\theta) + \frac{11}{16}r^5P_5(\cos\theta) + ...\right] + \\ \frac{T_2M_0\gamma}{T_1+T_2}\beta_1(t_1) \end{array}\right\} \tag{109}$$

3.0 Results and Discussion

The solution obtained in equation (109) was used to plot the graphs of the two fluids under consideration. These are hydrogen gas and paraffin oil using Maple 17 software. The plotting was done with the Magnetization (M_y), plotted against angle of inclination (θ) and radial adjustment (r). Figures 3.1a to 3.12a depict the graphs of hydrogen gas while Figures 3.1b to 3.12b depict the graphs of paraffin oil with varying radial adjustments.

International Journal of Mathematical Sciences and Optimization: Theory and Applications
10(3), 2024, Pages 10 - 30
https://doi.org/10.5281/zenodo.13152986

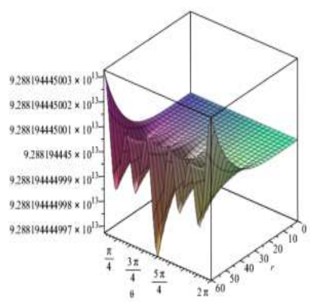

Figure 3.1a: Plot of M_y against $(\theta = 0..2\pi)$ and $r = 0..60$ for Hydrogen gas

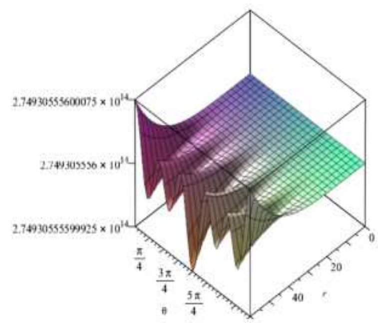

Figure 3.1b: Plot of M_y against $(\theta = 0..2\pi)$ and $r = 0..60$ for Paraffin Oil

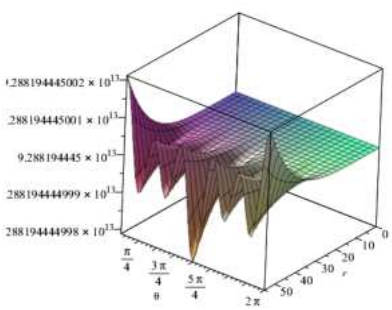

Figure 3.2a: Plot of M_y against $(\theta = 0..2\pi)$ and $r = 0..55$ for Hydrogen gas

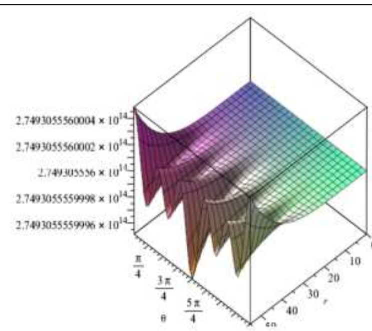

Figure 3.2b: Plot of M_y against $(\theta = 0..2\pi)$ and $r = 0..55$ for Paraffin Oil

International Journal of Mathematical Sciences and Optimization: Theory and Applications
10(3), 2024, Pages 10 - 30
https://doi.org/10.5281/zenodo.13152986

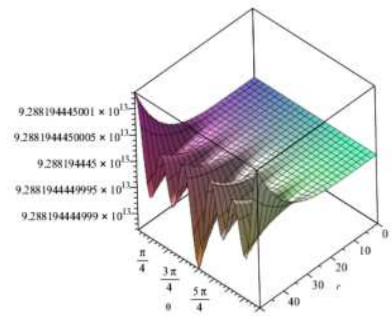

Figure 3.3a: Plot of M_y against $(\theta = 0..2\pi)$ and $r = 0..50$ for Hydrogen gas

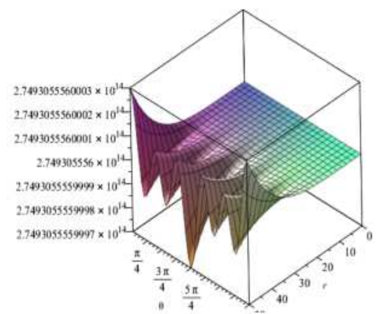

Figure 3.3b: Plot of M_y against $(\theta = 0..2\pi)$ and $r = 0..50$ for Paraffin Oil

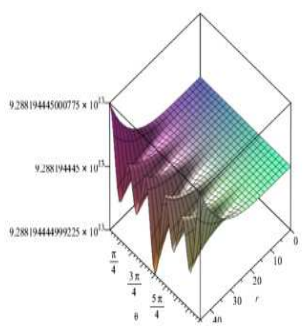

Figure 3.4a: Plot of M_y against $(\theta = 0..2\pi)$ and $r = 0..45$ for Hydrogen gas

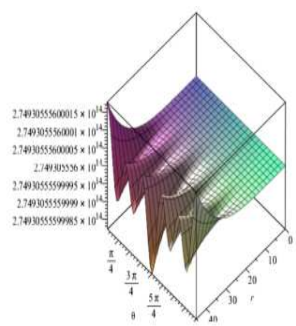

Figure 3.4b: Plot of M_y against $(\theta = 0..2\pi)$ and $r = 0..45$ for Paraffin Oil

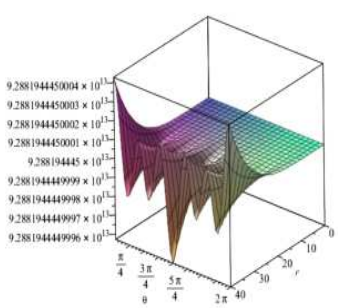

Figure 3.5a: Plot of M_y against $(\theta = 0..2\pi)$ and $r = 0..40$ for Hydrogen gas

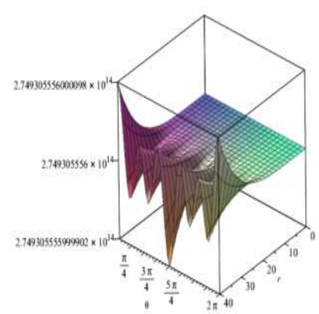

Figure 3.5b: Plot of M_y against $(\theta = 0..2\pi)$ and $r = 0..40$ for Paraffin Oil

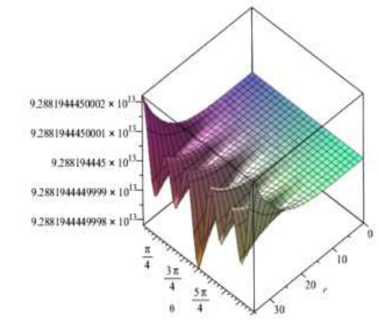

Figure 3.6a: Plot of M_y against ($\theta = 0..2\pi$) and $r = 0..35$ for Hydrogen gas

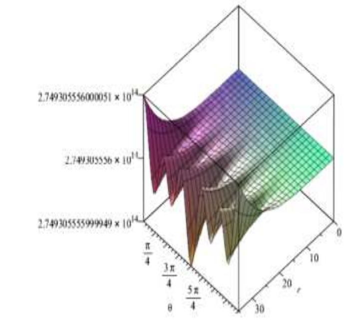

Figure 3.6b: Plot of M_y against ($\theta = 0..2\pi$) and $r = 0..35$ for Paraffin Oil

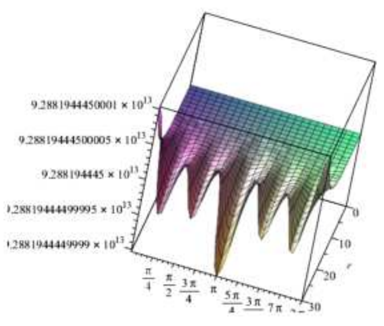

Figure 3.7a: Plot of M_y against ($\theta = 0..2\pi$) and $r = 0..30$ for Hydrogen gas

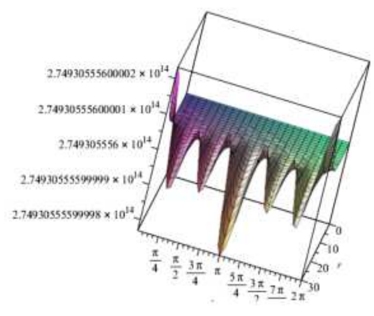

Figure 3.7b: Plot of M_y against ($\theta = 0..2\pi$) and $r = 0..30$ for Paraffin Oil

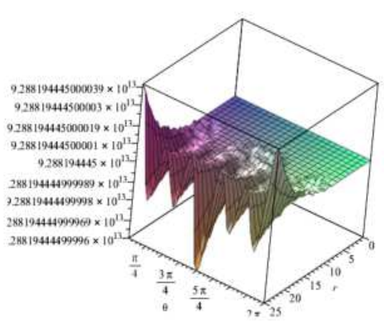

Figure 3.8a: Plot of M_y against ($\theta = 0..2\pi$) and $r = 0..25$ for Hydrogen gas

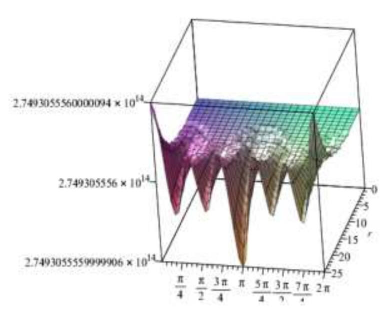

Figure 3.8b: Plot of M_y against ($\theta = 0..2\pi$) and $r = 0..25$ for Paraffin Oil

International Journal of Mathematical Sciences and Optimization: Theory and Applications
10(3), 2024, Pages 10 - 30
https://doi.org/10.5281/zenodo.13152986

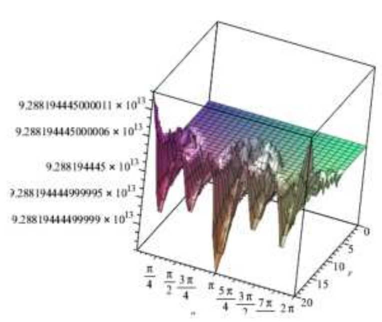

Figure 3.9a: Plot of M_y against $(\theta = 0..2\pi)$ and $r = 0..20$ for Hydrogen gas

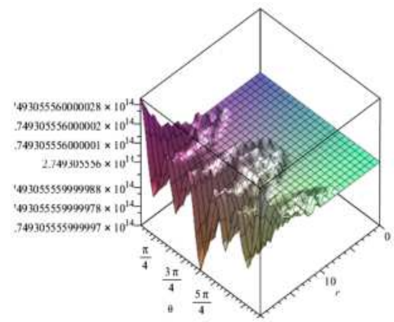

Figure 3.9b: Plot of M_y against $(\theta = 0..2\pi)$ and $r = 0..20$ for Paraffin Oil

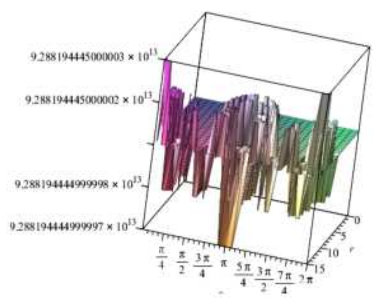

Figure 3.10a: Plot of M_y against $(\theta = 0..2\pi)$ and $r = 0..15$ for Hydrogen gas

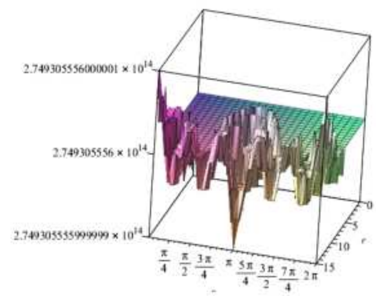

Figure 3.10b: Plot of M_y against $(\theta = 0..2\pi)$ and $r = 0..15$ for Paraffin Oil

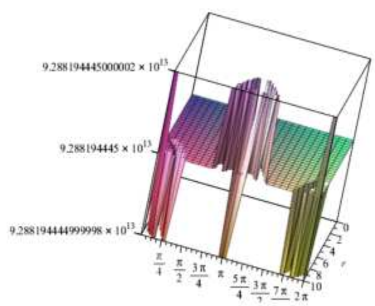

Figure 3.11a: Plot of M_y against $(\theta = 0..2\pi)$ and $r = 0..10$ for Hydrogen gas

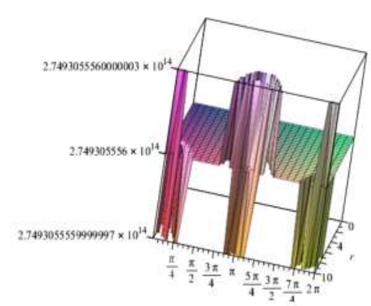

Figure 3.11b: Plot of M_y against $(\theta = 0..2\pi)$ and $r = 0..10$ for Paraffin Oil

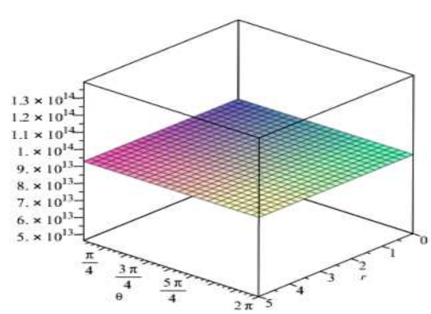

Figure 3.12a: Plot of M_y against $(\theta = 0..2\pi)$ and $r = 0..5$ for Hydrogen gas

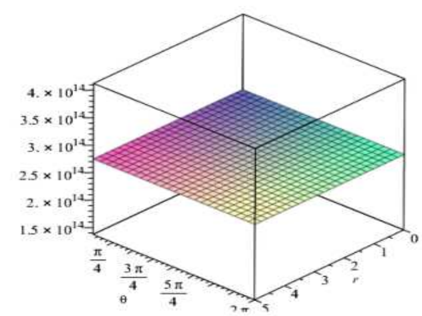

Figure 3.12b: Plot of M_y against $(\theta = 0..2\pi)$ and $r = 0..5$ for Paraffin Oil

International Journal of Mathematical Sciences and Optimization: Theory and Applications
10(3), 2024, Pages 10 - 30
https://doi.org/10.5281/zenodo.13152986

4.0 Conclusion

The general MRI flow equation has been solved in a spherical region. The fluids considered in this research work are hydrogen gas (compressible fluid) and paraffin oil (incompressible fluid).
The method of separation of variables adopted in spherical region led to Legendre equation of the first and second kinds. The forcing function added to the equation represents the radio-frequency field to perturb the particles of the fluids. This perturbation is the principle underlying the application of magnetic resonance imaging. As the fluid is introduced to the static magnetic field, the particles immediately align in the z-direction, hence the motion of the particles thereon is constant or uniform. When they are perturbed, they undergo precession and later relax at their unique relaxation times. During this process, they evolve echo which are read as signals. The signals which are interpreted by machines contain useful information on the particles being considered non-invasively. This is magnetization of the body or its response under MRI.
From the graphs in Figure 3.1a - 3.12a for hydrogen gas, it can be concluded that hydrogen gas responded with its value of Magnetization ranging from $9.28819444503 \times 10^{13}$ to 9.35×10^{14}. However, appreciable change is observed when magnetization is $9.2881944500003 \times 10^{13}$. This is because hydrogen gas is compressible and the essence of radial adjustment is to create an avenue for the particles of the gas to experience more vigorous collision that will enable the MRI machine register the signals appreciably. However, for paraffin oil, Figure 3.1b - 3.12b show that the value of Magnetization ranges from $2.749305556000075 \times 10^{14}$ to 2.75×10^{14} with observable appreciable change noticed when magnetization is $2.7493055560000094 \times 10^{14}$. These readings do not show much difference because it is an incompressible fluid as compared to compressible hydrogen gas which shows.
The analytical solution of Diffusion MRI equation adopted in this research work has shown the difference in response of compressible (hydrogen gas) and incompressible (paraffin oil) fluids through their different values for magnetization.

Acknowledgement
The authors of this paper sincerely appreciate the efforts of reviewers of this research paper. The observations pointed out have not only been carried out but have also enriched the paper. Your comments and observations have made significant impact on our capacity in writing research paper.
Declarations of Interest: The authors declare no competing financial interest.

References

[1] D. G. Nishimura. *Principles of Magnetic Resonance Imaging* . stanford: Stanford university press. 1996.

[2] M. Dada, O. B. Awojoyogbe, M. Hasler, K. B. Ben-Mahmoud, and A. Bannour. Establishment of a chebyshev-dependent inhomogeneous second order differential equation for the applied physics-related boubaker -turki polynomials. applications and applied mathematics: *An International Journal of (AAM), 3(6), 329-337*, available at http://pvamu.edu/aam. 2008.

[3] H. Singh and H. M. Srivastava. Numerical simulation for fractional-order bloch equations

arising in nuclear magnetic resonance by using jacob- polynomials. *MDPI Journal of Applied Sciences, 10(2850), 1-18, doi: 10.3390/app10082850* . 2020.

[4] K. Murase and N. Tanki. Numerical solutions to the time-dependent bloch equations revisited. *Journal of Magnetic Resonance Imaging, 29,126-131, doi: 10.1016/j.mri.2010.07.003*. 2010.

[5] O. B. Awojoyogbe, O. M. Dada, O. P. Faromika, and O. E. Dada. Mathematical concept of bloch flow equations for general magnetic resonance imaging: A review. *Wiley Online Library (wileyonlinelibrary.com), 38A (3), 85-101, Doi:10.1002/cmr.a.20210*. 2011.

[6] S. I. Yusuf, Y. M. Aiyesimi, O. B. Awojoyogbe, and O. M. Dada. Magnetic resonance imaging of plaques in a cylindrical channel. *Journal of Science, Technology, Mathematics and Education, 15(2), 74-82*. 2019a.

[7] S. I. Yusuf, Y. M. Aiyesimi, M. Jiya, O. B. Awojoyogbe, and O. M. Dada. Mathematical analysis of discontinuities in the flow field of gas in a cylindrical pipe using diffusion mri. *Nigeria Journal of Technological Research. 14 (2) https://dx.doi.org/10.4314/njtr.v14i2.9*. 2019b.

[8] M. Dada, O. B. Awojoyogbe, K. Boubaker, and O. S. Ojambati. Bpes analyses of a new diffusion-advection equation for fluid flow in blood vessels under different bio-physico-geometrical conditions. *Journal of Biophysics and Structural Biology, 2(3), 28-34, Available online at http://www.academicjournals.org/jbsb*. 2010.

[9] S. I. Yusuf, Y. M. Aiyesimi, and O. B Awojoyogbe. An analytical investigation of bloch nuclear magnetic resonance flow equation for the analysis of general fluid flows. *Nigeria Journal of Mathematics and Applications, 20, 82-92*. 2010.

[10] D. O. Olaoye, S. I. Yusuf, and Abdulraheem O. J. Analysis of t1 and t2 relaxation times from bloch equations for the estimation of age of human organs. a paper presented at the school of physical sciences biennial international conference (spsbic) 2021, page 487 - 499, october, 2021. 2021.

[11] S. I. Yusuf, Y. M. Aiyesimi, Jiya M., and O.B. Awojoyogbe. Analysis of partial and total blockage of unused engine oil in a radially symmetric cylindrical pipe using diffusion magnetic resonance equation. a paper presented at the 26th annual colloquium and congress of the nigerian association of mathematical physics. page 94, november, 2015. 2015.

[12] I. L. Ferreira, A. Garcia, and A. L. Moreira. On the transient atomic/heat diffusion in cylinders and spheres with phase change: A method to derive closed form solutions. *International Journal of Mathematics and Mathematical Sciences, 1-19, Doi: https://doi.org/10.1155/2021/6624287* . 2021.

[13] D. Datta and T. K Pal. A lattice bottzmann scheme for diffusion equation in spherical coordinates.*International Journal of Mathematics and Systems Science, 1, 1-4, Doi:10.24294/ijmss.v1i4.815.* 2018.

[14] A Gharehbaghi. Third and fifth-order finite volume scheme for advection- diffusion equation with variable coefficients in semi-infinite domain. *Water and Environmental Journal, 1-10, Doi:10.1111/wej.12233*. 2017.

International Journal of Mathematical Sciences and Optimization: Theory and Applications
10(3), 2024, Pages 10 - 30
https://doi.org/10.5281/zenodo.13152986

[15] L. A. Belyaev, A. S. Zaitsev, and Shevelev S. A. and Valkov E. P. Kondakov, A. A., and A. A. Matveeva. Numerical analysis of fluid particles motion in curved ducts. *MATEC Web of Conferences, 37, 1-4, Doi:10.1051/matecconf/20153701007.* 2015.

[16] E. O. Fatumbi. and O. J. Fenuga. Mhd micropolar fluid over a permeable streching sheet in the presence of variable viscosity and thermal conductivity with soret and duffour effects. *International Journal of Mathematical Analysis and Optimization: Theory and Applications. Vol. 2017, Pp. 211-232.* 2018.

[17] H. A. Isede, A. Adeniyan, and O. O. Oladosu. Entropy optimization and heat transfer analysis of mhd heat generating fluid flow through an anisotropic porous parallel wall channel: An analytic solution. *International Journal of Mathematical Analysis and Optimization: Theory and Applications. Vol. 9, No. 1, Pp. 81 - 103. . Doi: https://Doi.org/10.5281/zenodo.8218016.* 2023.

[18] A. O. Popoola, I. G. Baoku, and B. I. Olajuwon. Heat and mass transfer on mhd viscous-elastic fluid flow in the presence of thermal diffusion and chemical reaction. *International Journal of Heat and Technology, 34(1), 15-26, doi:10.18280/ijht.340103.* 2016.

[19] D. Eli and H. O. Aboh. Advective-nmr model of blood vessels with changing dimensions. *Nigerian Journal of Physics, 26(1), 99-105, Available at www.njpng.org.* 2015.

[20] D. Mallin, C. Fiedler, and A. Vesci. Analysis of mineral oil and glycerine through . retrieved from: https://www.semanticscholar.org/paper/anailsis-of-mineral-oil-and-glycerin-through- nmr-mallin-fiedler/e67684339985facd482 7801ec7d810231dca0db. 2011.

[21] A. J. Olaide, E. Olugbenga, and D. Abimbola. A review of the application of nuclear magnetic resonance in petroleum industry. *International Journal of Geosciences, 11, 145-169, Doi: 10.4236/ijg.2020.114009.* 2020.

[22] O. B. Awojoyogbe. Analytical solution of the time – dependent bloch nmr flow equations. *A Translational Mechanical Analysis. Physica A: Statistical Mechanics and its Applications, Volume 339, Issues 3–4, 2004, Pages 437-460, ISSN 0378-4371, https://doi.org/10.1016/j.physa.2004.03.061.* 2004.